

Rehman**Solar Potential Assessment of Facades in an Urban Context:
An Algorithm for 1.5D Digital Surface Models**Naveed ur Rehman¹, Timothy Anderson¹ and Roy Nates¹¹*Department of Mechanical Engineering, Auckland University of Technology, Auckland, New Zealand**E-mail: timothy.anderson@aut.ac.nz***Abstract**

An algorithm for estimating solar energy potential of facades in an urban context is proposed in this paper. The potential is presented in terms of the ratio of direct solar energy accumulated on facades when shadowing effects of nearby buildings are considered and to an ideal scenario when these shadowing effects are ignored. In achieving this, the algorithm utilizes a 1.5D Digital Surface Model (DSM) aligned with lines of latitude. On this basis, it is able to assess daily and year round potential during times when the sun is at solar noon. The algorithm is designed to be easily converted into a computer program. Also, the time and computer memory required for the assessment is independent of the complexity of a given relief. To illustrate the algorithm, three case studies considering hypothetical DSM's of equal façade surface areas, located in Auckland (New Zealand), are presented and compared with each other.

1. Introduction

Due to the high upfront cost and low conversion efficiency of photovoltaic (PV) panels, it is prudent to measure or estimate the accessibility of solar radiation at an installation site before deployment (Rehman and Siddiqui, 2015; Rehman and Siddiqui, 2016). Traditionally, domestic-size solar PV power plants have been developed with a view to partially meeting the electricity requirements when installed on the rooftop of a dwelling with good solar access, such as a free-standing house in a relatively low population density area/suburb. On this basis, many of the state-of-the-art solar potential estimation methodologies and tools that have been developed are focused on assessing the solar potential of horizontal (or moderately inclined) surfaces (Hofierka et al., 2002; Wiginton et al., 2010; Nguyen and Pearce 2012; Brito et al., 2012; Jakubiec and Reinhart, 2013). Such methods make use of digital surface models (DSM) of given urban relief, represented by a geo-referenced x-y plane with data values expressing physical elevation of locations. Approaches used in these methods are based on choosing points on surfaces and calculating the sky and sun-path obstructions due to urban features around, when viewed from these points.

However, when most of the population is residing in high population density urban areas where features have started to propagate more and more vertically, the available rooftop area of such buildings has become a significant constraint to the installation of these power plants. Façades, on the other hand, cover a much larger area of building than rooftops and certainly, they can be used for installing PV panels. Unfortunately, the existing methodologies are not well suited to estimates of solar radiation on vertical elements even when they are adapted for this purpose. One of the main reasons is the inherent characteristic associated with their use of DSM, where a façade is represented by only the highest points along its periphery.

Now, deploying solar potential algorithms on, what is effectively, an infinite number of points on a façade's exposed surface is impractical. Even if fewer hyperpoints are chosen, the large number of façades across a full cityscape (such as Auckland with an area $>4000 \text{ km}^2$) is prone to consume substantial computational resources and time. However, poor resolution may result in highly unrealistic and unreliable estimates (Freitas et al., 2015). Therefore, the development of efficient and accurate methodologies for assessing solar potential on façades are required to better inform the design of façade integrated PV systems (Carneiro et al., 2010; Redweik et al., 2011; Hofierka and Zlocha, 2012) at a city wide scale. Furthermore, developing an approach that is independent of choosing hyperpoints for assessing solar potential of façades, together with a faster, less memory intensive and reliable algorithm, would definitely be a significant contribution. As such, this work presents a novel approach to achieving this, along with a compatible shadowing algorithm using a 1.5D DSM to describe an urban relief.

2. Methodology

A typical simplified DSM employed in this study, as a key input describing urban features of a relief, is shown in Figure 1. This DSM consists of a number (i_o) of vertical features, each denoted by i , aligned with lines of latitude, similar to buildings aligned to a streetscape flowing east to west. The centre distance between each feature is d (m) and the height and width of each feature are h_i (m) and W (m), respectively.

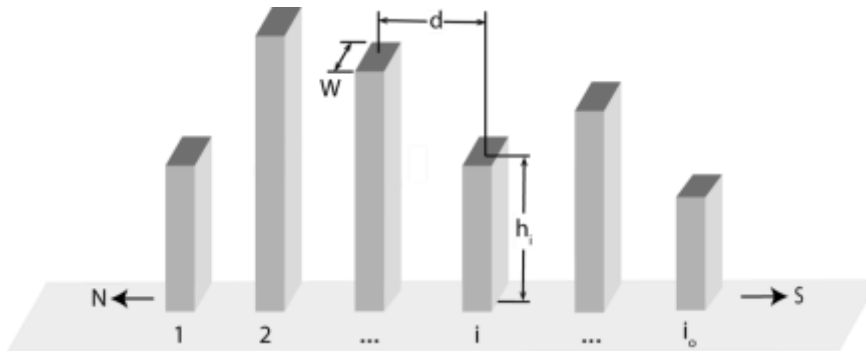


Figure 1. Nomenclature of a typical 1.5D DSM describing urban features of a relief

Now, beam radiation reaching the earth surfaces arrives an angle α relative to the local horizontal, which is equal to the elevation angle of sun. At noon of any n^{th} day of the year, this angle can be obtained by (1):

$$\alpha_n = 90 - \phi + \delta_n \quad (1)$$

Where ϕ (deg) is latitude angle of site and δ_n (deg) is declination angle, such that:

$$\delta_n = 23.45 \sin\left(360 \frac{284 + n}{365}\right) \quad (2)$$

Considering the urban features in the DSM and the sun's elevation angle, the height of the shadow on i^{th} feature due to $(i - 1)^{\text{th}}$ feature can be obtained by considering the trapezoid $abcd$, shown in Figure 2. As that s_i (m) is the height of shadow, given by (3):

$$s_i = h_{i-1} - d \tan(\alpha_n) \quad (3)$$

However, Eq. (3) is valid only as long as the height of the shadow on the $(i - 1)^{\text{th}}$ feature, due to the feature located prior to it, is less than the height of that feature (see for example Feature e in Figure 2).

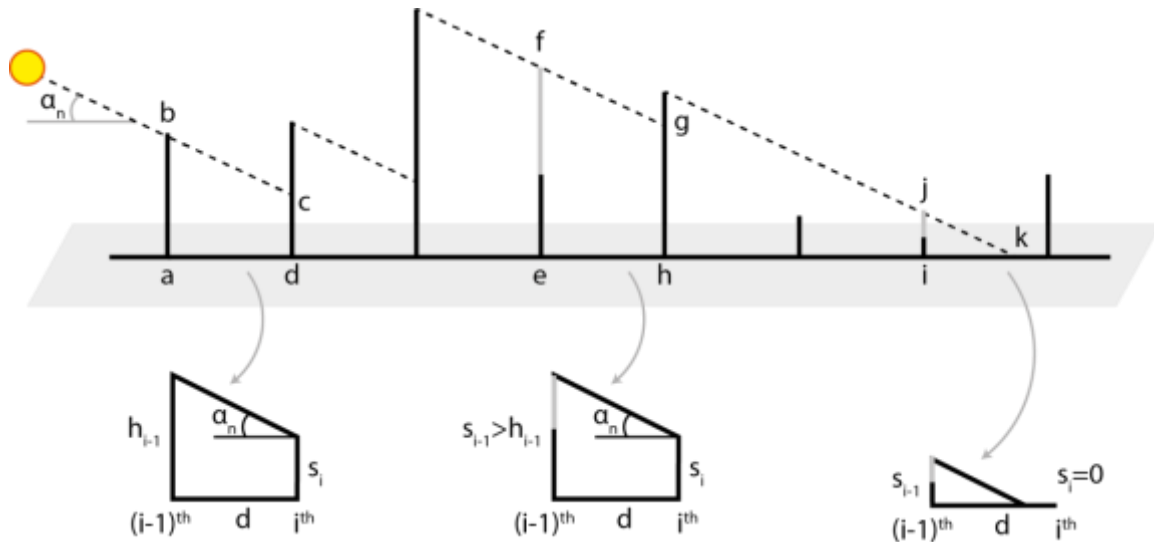


Figure 2. Shadow cast on features due to sunlight obstructed by the preceding features

To account for a situation when the height of a shadow point at preceding a feature could be more than the height of that feature itself ($efgh$ in Figure 2), Eq. (3) would require the following modification:

$$s_i = \max(h_{i-1}, s_{i-1}) - d \tan(\alpha_n) \quad (4)$$

Where, the *max* function implies the need to pick either the height of preceding feature, or the height of the shadow point above that preceding feature, whichever is greater.

In circumstances when the length of shadow cast by a feature is not long enough to reach the following feature, Eq. (4) will result in an unrealistic negative value. This is illustrated by triangle ijk in Figure 2. To accommodate this situation, Eq. (4) can be modified to yield a minimum value of zero:

$$s_i = \max(0, \max(h_{i-1}, s_{i-1}) - d \tan(\alpha_n)) \quad (5)$$

After obtaining the height of the shadow on every feature, the unshaded height of these features can be obtained. Two cases should be considered: firstly, if the height of feature is less than the shadow height above that feature then there would be no unshaded height, and secondly, if the shadow height on that feature is less than the height of feature, the difference between the heights will be the unshaded height. Mathematically, both cases can be expressed in a single equation as:

$$h'_i = h_i - \min(h_i, s_i) \quad (6)$$

Where the *min* function implies taking the smaller value of the two in parenthesis.

Following on from this, the beam radiation received by an i^{th} feature at noon of some n^{th} day (I_i , Watts) depends upon: the incident solar beam irradiance (G_n , W/m^2), the elevation angle of the sun and the unshaded area of that feature, as shown in Figure 3. This can be calculated as:

$$I_{i,n} = G_n \cos(\alpha_n) W h'_{i,n} \quad (7)$$

The sum of the aforesaid solar radiation values, for all features, will yield the total beam radiation received by the vertical elements of given urban relief at noon of any particular day of the year:

$$I_n = \sum_i I_{i,n} = G_n \cos(\alpha_n) W \sum_i h'_{i,n} \quad (8)$$

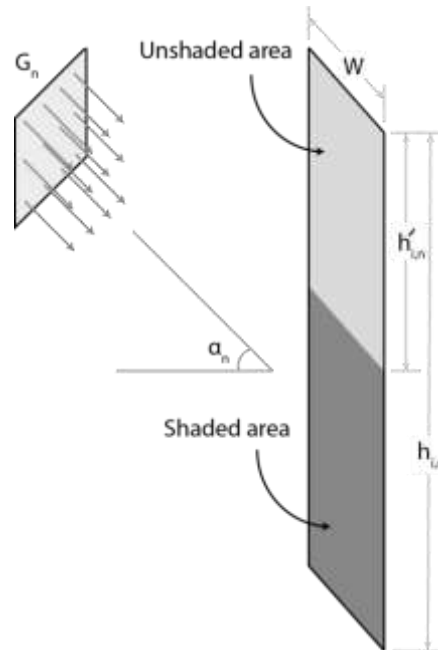


Figure 3. Solar radiation reaching the surface of a partially shaded feature

In turn, this can be compared to the maximum solar radiation that could be received by the given urban relief, at noon of same day, in the event that there were no shadows. Such that:

$$I_{n,max} = G_n \cos(\alpha_n) W \sum_i h_i \quad (9)$$

As such, the ratio of I_n to $I_{n,max}$ represents an instantaneous spatiotemporal measure of the solar energy potential (P_n) of an entire urban relief:

$$P_n = \frac{\sum_i h'_{i,n}}{\sum_i h_i} \quad (10)$$

Therefore, Eq. (10) can be used to determine the performance (degree of solar access) of a given urban relief for any day of the year. A well-planned relief would have values of P_n close to 1.0 for most of the days of year, meaning that all facades had good access to beam radiation. Correspondingly, the year-round solar potential (P) could be obtained by taking the average of Eq. (10) over all the days of a year:

$$P = \frac{\sum_n P_n}{\sum_n n} \quad (11)$$

This relation would be helpful in comparing the performance of different reliefs at a macroscale.

3. Results and Discussion

Three hypothetical layouts, virtually located in Auckland ($\phi = 36.85^\circ S$), were established for the simulation and comparison purposes, as shown in Figure 4. Each layout consisted of eight features, separated by a distance of $d = 0.5m$. In DSM-1, the height of all features was assumed to be equal. In DSM-2, taller features were placed towards the true North where the sun would be found at noon, while DSM-3 was the reversed case of DSM-2, with taller features placed further south. To ensure an even comparison, it was assumed that the sum of the heights of all features in each layout were equal, as listed in Table 1.

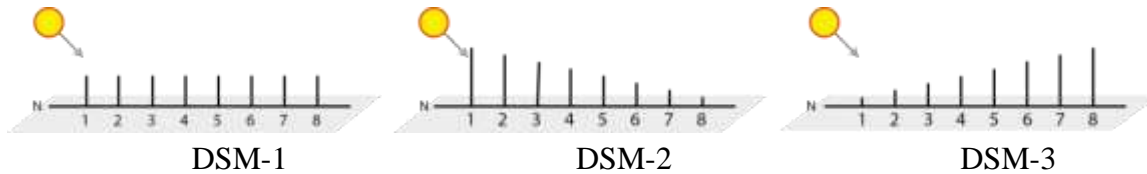


Figure 4. Three different hypothetical DSM layouts used for simulation and comparison purposes

Table 1. Heights of features in three different DSMs, considered for simulation and comparison purposes

Feature # (<i>i</i>)	Height of feature (h_i , m)		
	DSM-1	DSM-2	DSM-3
1 (North)	1.00	2.00	0.03
2	1.00	1.71	0.28
3	1.00	1.42	0.57
4	1.00	1.14	0.85
5	1.00	0.85	1.14
6	1.00	0.57	1.42
7	1.00	0.28	1.71
8 (South)	1.00	0.03	2.00
$\sum h_i$	8.00	8.00	8.00

Subsequently the daily potential of each DSM layout, obtained after performing simulations for all days of year, was found and is shown in Figure 5. From this it can be seen that for days in summer (Oct-Feb), when sun elevation angle is comparatively high, the daily potential of DSM-1 is highest. This was perhaps somewhat obvious, as the shadows cast by the features in DSM-1 were not able to reach the subsequent features, but this serves as illustration. Conversely, during the same period (and also during winter), the taller features towards north in DSM-2 cast long shadows that easily reached the subsequent features, hence the daily potential was found to be the minimum.

Now during the summer months, DSM-3 performed better than DSM-2 because of the shorter features towards north, but worse than DSM-1 because of the few taller features towards the south. However, during winter when the sun elevation angle is fairly low, DSM-3 was found to perform better than both other configurations. This was again because of having smaller features towards north.

Using the solar potential as a metric for comparison, the year-round performance of DSM-1, 2 and 3 were found to be 71%, 58% and 72%, respectively. In other words, urban layouts with shorter buildings towards north (in the southern hemisphere), are recommended for the best solar potential.

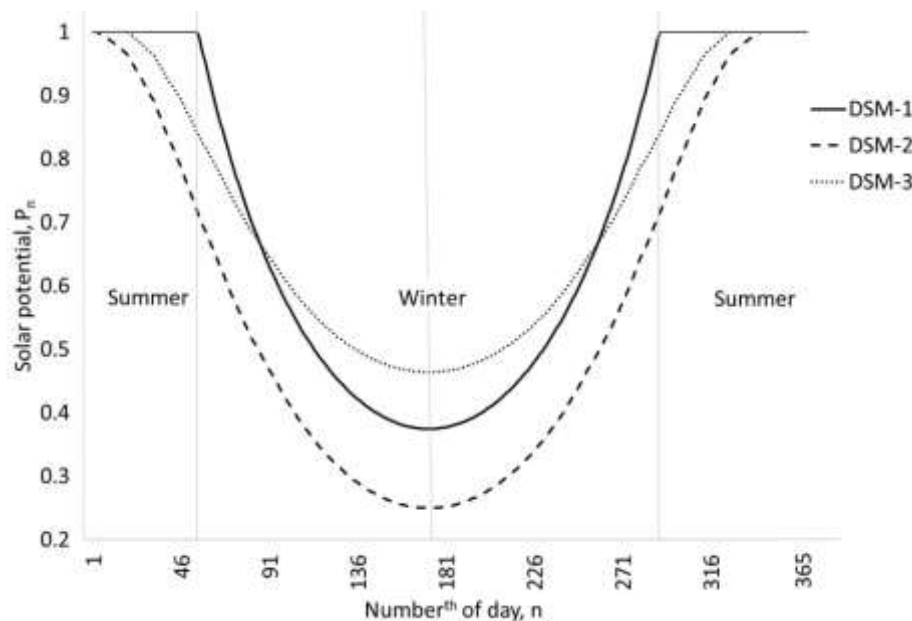


Figure 5. Comparison of daily solar potential of façades for different layouts

4. Conclusion

A novel approach for estimating solar energy potential of facades in an urban context along with a compatible shadow algorithm has been proposed. This approach is independent of choosing hyperpoints on the vertical surfaces of walls. For the daily potential of a complete urban relief, the proposed relation is mainly the ratio of sum of shaded heights to the sum of total heights of all façades. The year-round potential is the integral of daily potentials over sum of days in year. Simulations were performed for the three hypothetical layouts of DSMs, virtually located in Auckland (New Zealand). It was found that the façades in urban layouts having shorter buildings towards north perform better in terms of their solar radiation collection potential. This provides obvious insights to urban planners considering the future potential for façade integrated PV power systems.

References

- Brito, M., Gomes, N., Santos, T. and Tenedrio, J, 2012, 'Photovoltaic potential in a Lisbon suburb using LiDAR data' *Solar Energy*, 86(1), p283-288.
- Carneiro, C., Morello, E., Desthieux, G., and Golay, F, 2010, 'Urban environment quality indicators: application to solar radiation and morphological analysis on built area', *Proceedings*

of the 3rd WSEAS international conference on Visualization, imaging and simulation, p141-148.

Freitas, S., Catita, C., Redweik, P. and Brito, M, 2015, 'Modelling solar potential in the urban environment: State-of-the-art review', *Renewable and Sustainable Energy Reviews*, 41, p915931.

Hofierka, J. and Suri, M, 2002. 'The solar radiation model for Open source GIS: implementation and applications', *Proceedings of the Open source GIS-GRASS users conference*, p51-70.

Hofierka, J. and Zlocha, M, 2012, 'A New 3-D Solar Radiation Model for 3-D City Models', *Transactions in GIS*, 16(5), p681-690.

Jakubiec, J. A. and Reinhart, C. F, 2013, 'A method for predicting city-wide electricity gains from photovoltaic panels based on LiDAR and GIS data combined with hourly Daysim simulations', *Solar Energy*, 93, p127-143.

Nguyen, H. T. & Pearce, J. M., 2012. Incorporating shading losses in solar photovoltaic potential assessment at the municipal scale. *Solar Energy*, 86(5), pp. 1245-1260.

Redweik, P., Catita, C., Brito, M. C., and Grande, C., 2011, 'PV potential estimation using 3D local scale solar radiation model based on urban LIDAR data', *Proceedings of the ISPRS Workshop High-Resolution Earth Imaging for Geospatial Information, Hannover, Germany*, p5-9.

Rehman, N. U. and Siddiqui, M. A, 2015, 'A novel method for determining sky view factor for isotropic diffuse radiations for a collector in obstacles-free or urban sites', *Journal of Renewable and Sustainable Energy*, 7(3).

Rehman, N. U. and Siddiqui, M. A, 2016, 'A novel methodology for determining sky blocking by obstacles viewed virtually from any location on site', *Energy and Buildings*, 128, p827-833.

Wiginton, L., Nguyen, H. and Pearce, J., 2010, 'Quantifying rooftop solar photovoltaic potential for regional renewable energy policy', *Computers, Environment and Urban Systems*, 34(4), p345-357.

Appendix "Computer Program Design"

```

Set d,  $\phi$ , n      %% Assign data as per given DSM, location & numberth of day
Calculate  $\delta = 23.45 * \sin ( 360 * ( 284 + n ) / 365)$       %% Eq (1)
Calculate  $\text{Alpha} = 90 - \phi + \delta$  %% Eq (2)
Set Feature_Heights = array(1,5,3,6,8,4,...)                %% Assign data as per given
DSM
Set h_dash = Empty Array
Set io = count ( Feature_Heights )
Set i = 1
While i is less than or equals to io if
i is greater than 1 then
    Set h = Feature_heights ( i )      s = max( 0 , max( ho , so
) - d*tan( Alpha )) %% Eq (5)
    Set h_dash( i ) = h - min( h , s )      %% Eq (6)
End-of-If
Set ho = h, so = s, i = i + 1
End-of-While
Print all values of h_dash array
Sum_h = sum( h )
Sum_h_dash = sum( h_dash )
Pn = Sum_h_dash / Sum_h      %% Eq (10) Print Pn

```

